JMEPEG (2012) 21:2316–2322
DOI: 10.1007/s11665-012-0202-7

1059-9495/$19.00

Influence of Additional Tensile Force on Springback of Tube Under Rotary Draw Bending

Daxin E, Zhiping Guan, and Jisheng Chen

(Submitted August 24, 2011; in revised form February 15, 2012)

According to the characteristics of tube under rotary draw bending, the formulae were derived to calculate the springback angles of tubes subjected to combined bending and additional tension. Especially, as the neutral layer (NL) moves to the inner concave surface of the bend, the analytical values agree very well with the experimental results. The analysis shows that the additional tensile force causes the movement of the NL toward the bending center and makes the deformation behavior under rotary draw bending or numerically controlled (NC) bending different with that under pure bending, and also it could enlarge the springback angle if taking the movement of the NL into consideration. In some range, the springback angle would increase slightly with larger wall thickness/diameter ratio and decrease with wall thinning. The investigation could provide reference for the analysis of rotary draw bending, the design of NC tube bender and the related techniques.

Keywords additional tensile, rotary draw bending, springback

1. Introduction

Besides the increasingly wide application of tubular products in water transfer industry due to their hollow structure, the application of tubes become wider and wider in engineering (especially transportation vehicles) owing to light weight, low material utilization, and high energy absorption capability compared to other structures with the same stiffness and intensity. It is necessary to explore the bending mechanism of tube and many other issues related to the formation and control of flaws (Ref 1-6). In addition, Al-Qureshi (Ref 7, 8) had elastic-plastic analysis on tube bending, and calculated the bending moment with upper limit method, and then put forward a method to quantitatively predict springback and residual stresses. Ghosh et al. (Ref 9, 10) revealed that the relationship of stress-strain following unloading was nonlinear and hence presented a concept of springback modulus changing with the severity of plastic deformation, but earned little attention. Megharbel et al. (Ref 11) had elastic-plastic bending analysis of tubes with some different cross-sectional shapes, but the precisions of analytical results were not high. Murata et al. (Ref 12) studied the influence of strain harden index (n) on the ovalization of cross section for some tubes with different materials by utilizing experiments and simulations. E and Liu (Ref 13) found that the bending springback of tube consists of instantaneous springback and time-dependent springback for

Daxin E and **Jisheng Chen**, School of Materials Science and Engineering, Beijing Institute of Technology, No. 5, South Street of Zhongguancun, Haidian District, Beijing 100081, China; and **Zhiping Guan**, Superplastic and Plastic Research Institute, Jilin University, Changchun 130022, China. Contact e-mail: daxine@bit.edu.cn.

Nomenclature

d_0	Original outer diameter of tube
d_1	Original inner diameter of tube
D	Linear hardening coefficient
E	Elastic modulus
F	Additional tensile force
I	Inertia moment of cross section
M	Applied bending moment
R	Curvature radius of the original central layer of tube,
R_i	Curvature radius of the inner concave surface of tube
r_0	Original outer radius of tube
r	Radius of any a point in cross section
r_m	Radius of the middle circle in the wall thickness
t	Wall thickness
t_0	Original wall thickness
Δt	Amount of wall thinning
A	Displacement angle related to the NL
ε_θ	Tangential strain
ε_F	Tensile strain caused by the tensile force F
ε_y	Strain corresponding to the original yield point
ε_t	Wall thickness strain
ε_{to}	Wall thickness strain in the outer convex portion of tube
ε_{ti}	Wall thickness strain in the inner concave portion of tube
σ_y	Original yield stress
σ_θ	Tangential stress
σ_F	Tensile stress caused by the tensile force F
ρ	Curvature radius of the NL
ρ'	Curvature radius of the NL after springback
θ	Bending angle
$\Delta\theta$	Springback angle
ξ	Offset of the NL to the central layer
Φ	Circumferential angle in cross section
ν	Poisson's ratio

1Cr18Ni9Ti stainless steel tubes, and derived the basic formulae for approximate calculation of springback. However, although they have played positive roles on studies of tube bending, all the investigations are confined to pure bending instead of considering the potential effects of bending modes and other externally applied forces. This results in the disconnection between theoretical analysis and practical manufacture (Ref 14-16). Moreover, the problems concerning springback are always keeping unsettled during exploring the mechanism of tube bending, and it restricts the development of precision bending and numerically controlled (NC) bending of tubes. Therefore, this study is carried out to analyze the influence of the neutral layer's (NL's) movement on springback through adding tensile force to pure bending based on the characteristics of tube under rotary draw bending or NC bending. It would provide reference for the investigation of bending mechanism and the development of NC bending technique of tubes.

2. Basic Assumptions on Rotary Draw Bending

(1) It is regarded as pure bending deformation to curl a tube alongside the bend die. And the direction of additional tensile force is tangent to bending arc. In analysis of springback, only the stresses and the strains along the tangential direction are considered.
(2) The tensile deformation and the bending deformation concur, namely the discrepancy of tension-bend (first tension and then bend) and bend-tension (first bend and then tension) is negligible.
(3) Due to the constraint of the grooves of the bend die and the clamp die, the outer diameter perpendicular to bending plane is changeless during tube bending, namely the effect of ovalization of tube's cross section is negligible.
(4) The materials of tubes are simplified as the linear hardening model, and the volume is uncompressible during tube bending, namely the Poisson's ratio ν is 0.5.
(5) For simplifying the calculation, the radial force of the bend die acting on the tube for balancing the tangential tensile force would not be considered.

3. The Deformation Analysis in Rotary Draw Bending

3.1 The Bending Test and Finite Element Analysis

The schematic diagrams of rotary draw bending and the involved die structure are presented in Fig. 1. For holding a work piece, both the clamp die and the bend die have grooves with arc length of lower than half-circle (almost 0.48 circumferences) and with diameter of slightly greater than the outer diameter of tube. While pulling the clamp die, the tube would be bent by rotating along with the bend die. For avoiding reverse displacement of the unbent portion of tube, the pressure die and the follower-type pressure die are designed to guarantee the unbent portion of tube to advance along tangential direction. For balancing the frictional forces between the surface of tube wall and the grooves of the pressure die and the wiper die, a tensile force F along tangential direction of bending arc need to be added near the bending point. At the beginning of bending, there exists a moment, whose direction is reverse to the applied bending moment, between the two portions of tube which contact the bending die and the pressure die, respectively. To reduce the complexity of analysis, the effect of this moment on bending is neglected. In a series of rotary draw bending tests of thin-walled tubes with small diameter, the materials of tubes involve 1Cr8Ni9Ti, 5A03 (aerial corrosion-resisting aluminum) and T2 (pure copper), and their wall thickness/diameter ratios t_0/d_0 range from 0.083 to 0.2. The mechanical properties of the materials from tensile tests are present in Table 1.

3.2 The Influence of the Additional Tensile Force on the Variation of Tube's Wall

In rotary draw bending test, the deformation zone was mainly localized at a small field around the tangent point of the unbent portion and the bent portion of tube. Under the pressing by the clamp die, no slip occurs between the outer concave surface of the bent tube and the groove of the bending die due to near-static friction. Thus, the unbent portion of tube would have a significant draw-bend deformation as it begins to move into the deformation zone under the additional tensile force. After a bent 1Cr18Ni9Ti tube with the bending angle of 180° and with the bending radius/tube diameter ratio R/d_0 of 3 was split in half along the center plane parallel to the bending plane, the wall thickness strains ($\varepsilon_t = \ln t/t_0$) on some characteristic points are measured by the precise universal tester. And based on the same conditions, finite element simulations were performed. Figure 2 describes the distribution of the wall thickness strains obtained by experiment and simulation. These results show that the absolute values of wall thickness strains in the outer convex portion of tube are remarkably greater than those in the inner concave portion of tube, namely $|\varepsilon_{to}| > \varepsilon_{ti}$. The strains in the middle portion of tube are large while those in

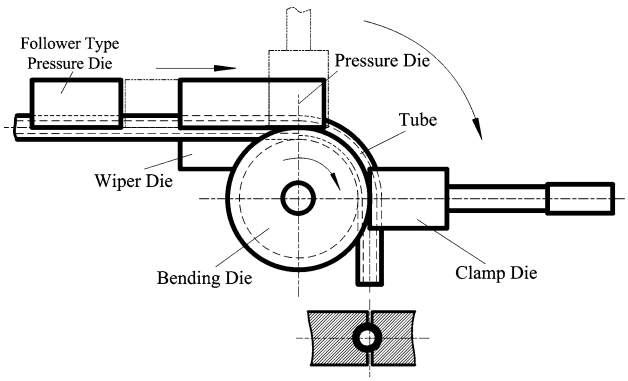

Fig. 1 The schematic diagrams of rotary draw bending and its die structure

Table 1 The mechanical properties of tube materials

Material	E, GPa	D, MPa	σ_y, MPa
1Cr8Ni9Ti	198	1080	205
5A03	73	275	80
T2	110	411	70

E, elastic modulus; D, linear hardening coefficient; σ_y, original yield stress

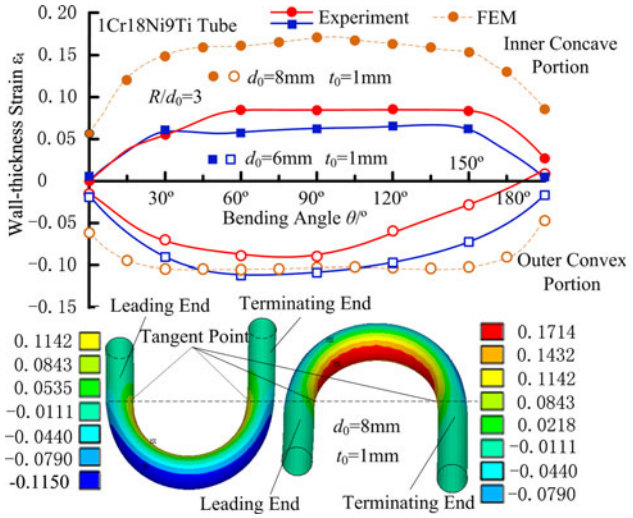

Fig. 2 The experimental and FEM results of wall thickness strains

the leading end and the terminating end are quite small. This tendency is unchangeable when the wall thickness/diameter ratio was varied. For the strains ε_{to} in the outer convex portion of tube, the FEM results agree well with the experimental data. However, for the strains ε_{ti} in the concave portion of tube, the FEM results are much greater than the experimental values. It is because the additional tensile force was not introduced into the finite element model and the decrease of the wall thickness deformation in the concave portion due to tangential tension was not considered in FEM (Ref 17).

Rotary draw bending should be a successive partial plastic deformation, which is mainly localized in the field around the tangent point of the unbent tube and the bending die. Except that the leading end and the terminating end of tube are subjected to radial pressing forces by the pressure die and the clamp die, respectively, the bent portion of tube plays the role of transferring forces during tube bending. Most of experimental results show that for the two ends of tube, not only the wall thickness strains are small but also the ovalizations of cross section are smaller than those of the middle section of tube. It is because the two ends of tube are subjected to radial pressing forces and there is some slip amount of the inner concave surface to the groove in the bending die, while the middle section of tube with no restriction would always endure the tangential tension (Ref 18).

3.3 The Stress-Strain Relation of Materials in Rotary Draw Bending

Figure 3 presents that the distribution of the tangential stress σ_θ in the transverse section of tube subjected to the bend moment M. Also in the right of Fig. 3, the stress-strain relation of materials with the linear hardening model follows as A′S′OSA lines approximately. Due to the effect of the rotation of the clamp die and friction of the pressure die, the tensile force F along tangential direction of bending arc is added into the deformation zone of tube, and the relevant states of stress and strain differ with pure bending. To simplify the analysis, it is assumed that all longitudinal fibers have uniform tension in any layer of tube. In tube bending, the amount of tangential tension in the outer convex portion of tube gradually increases and the tensile stress grows following as OSA lines under the combination of F and M. However, in the inner concave portion, the

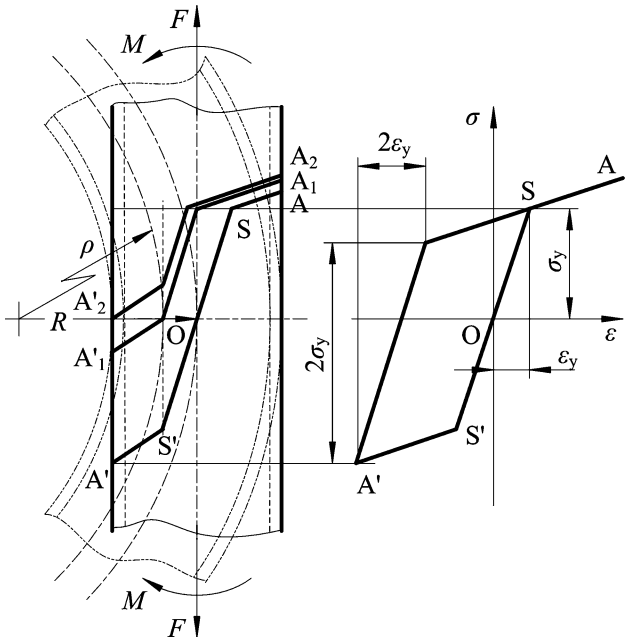

Fig. 3 The stress-strain distribution with the additional tensile force and the movement of the NL

additional tensile force F makes the compress stress caused by the bending moment recover elastically and decreases following Hook's law. Because all longitudinal fibers in the original central layer endure the tension, the NL (of strain) and the NL of stress would move toward the bending center (Ref 19).

When the tensile strain ε_F caused only by tensile force F reaches the strain ε_y which corresponds to the original yield point, the stress will change following A'_1A_1 lines. When the strain ε_F increases up to the absolute value of elastic component of the compress strain in the inner concave portion, the distribution of stresses in the transverse section is similar to A'_2A_2 lines. At the moment, theoretically, the NL of stress coincides with the inner concave surface of tube. However, if the hysteresis of strain and nonintegrality for elastic unloading are considered in analysis, the offset between the NL and the NL of stress will increase as the strain ε_F increases, namely the NL may still be located in the transverse section of tube. As the tangential stresses and strains continue to grow, the NL will coincide with the inner concave surface of tube while the NL of stress will move out of the transverse section of tube.

4. The Analysis of Springback in Rotary Draw Bending

4.1 The Springback when $\varepsilon_F < \varepsilon_y$

The geometry parameters of tube's cross section are shown in Fig. 4. The original outer diameter of tube is denoted by d_0 (=$2r_0$), and the original wall thickness is denoted by t_0. For any a point with the radius r, the nominal strain along the tangential direction of bending arc can be represented as

$$\varepsilon_\theta = \varepsilon_F + \frac{r \sin \varphi}{\rho} \qquad \text{(Eq 1)}$$

where ρ is the curvature radius of the NL.

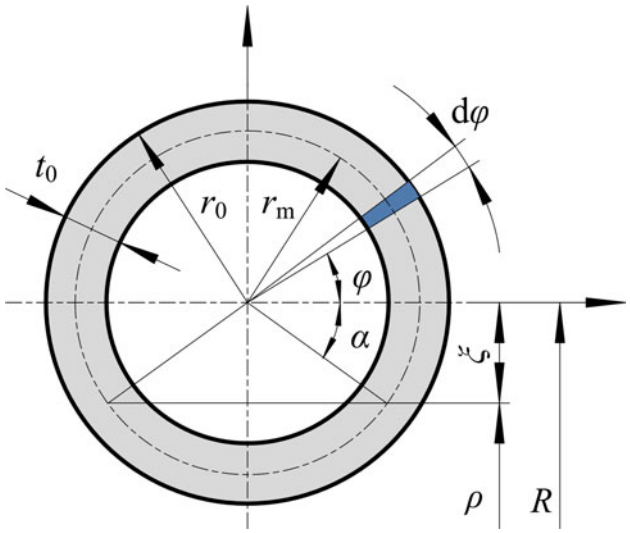

Fig. 4 The geometry of cross section of tube

In the section below the NL, it is considered that $r\sin\varphi \le 0$. Based on basic assumption 4, the total stress along the tangential direction is expressed as

$$\sigma_\theta = \sigma_y + D\varepsilon_\theta = \sigma_y + D\left[(\varepsilon_F - \varepsilon_y) + \frac{r\sin\varphi}{\rho}\right] = \sigma_y\left(1 - \frac{D}{E}\right) + \sigma_F\frac{D}{E} + D\frac{r\sin\varphi}{\rho}. \quad \text{(Eq 2)}$$

4.1.1 Neglect of the Movement of the NL. If the movement of the NL is not considered, namely the displacement angle α related to the NL is equal to zero and ρ is equal to R denoting the curvature radius of the original central layer of tube, the tangential stress can be expressed as

$$\sigma_\theta = \sigma_y\left(1 - \frac{D}{E}\right) + \sigma_F\frac{D}{E} + D\frac{r\sin\varphi}{R}. \quad \text{(Eq 3)}$$

In pure bending, when the effect of tiny elastic deformation in the both sides of the NL and the variation of wall thickness of tube are neglected, the applied bending moment can be given by

$$M = \int_0^{2\pi} \sigma_\theta r\sin\varphi r_m t d\varphi = \int_0^{2\pi}\left[\sigma_y\left(1 - \frac{D}{E}\right) + \sigma_F\frac{D}{E} + D\frac{r\sin\varphi}{R}\right] r\sin\varphi r_m t d\varphi = r_m t r D\frac{r}{R}\pi \quad \text{(Eq 4)}$$

where r_m is the radius of the middle circle in the wall thickness.

Because the recovery process after bending is the elastic deformation, the interrelation of σ_θ and ε_θ should obey Hook's law $\sigma_\theta = E\varepsilon_\theta$. From this, the following equation can be derived:

$$\frac{1}{\rho} - \frac{1}{\rho'} = \frac{M}{EI} \quad \text{(Eq 5)}$$

where ρ' is the curvature radius of tube after springback.

The bending angle of tube is denoted by θ, and the springback amount is denoted by recovery angle $\Delta\theta$, which is also called the springback angle, and it can be expressed by

$$\Delta\theta = \theta - \theta' = \left(1 - \frac{\rho}{\rho'}\right)\cdot\theta = \frac{\Delta(1/\rho)}{1/\rho}\cdot\theta = \frac{M\rho}{EI}\cdot\theta \quad \text{(Eq 6)}$$

where the inertia moment I of cross section can be calculated by

$$I = \frac{\pi}{64}\left(d_0^4 - d_1^4\right) = \frac{\pi}{2}t_0\left(r_0 - \frac{t_0}{2}\right)\left(2r_0^2 - 2r_0t_0 + t_0^2\right). \quad \text{(Eq 7)}$$

Substituting Eq 4 and 7 into 6, we can obtain the springback angle as follows:

$$\Delta\theta = \frac{M\rho}{EI}\cdot\theta = \frac{2D\frac{\rho}{R_0}r^2}{E\left(2r_0^2 - 2r_0t_0 + t_0^2\right)}\cdot\theta \quad \text{(Eq 8)}$$

In rotary draw bending, the tangential tensile force F resists the compress instability on the inner concave wall of tube. And due to restriction of the bending die's groove, the outer radius of the inner concave portion of tube is usually unchangeable. However, for the outer convex portion without restriction, the outer radius will decrease due to wall thinning even if the ovalization of tube's cross section would not occur in tube bending. When the amount of wall thinning is denoted by Δt, the outer radius can be expressed by $r \approx r_0 - \Delta t$. Thus, when it is assumed that $\rho = R$ without a consideration of the movement of the NL, Eq. 8 can be adjusted to

$$\Delta\theta = \frac{D}{E}\frac{1}{1 - \frac{t_0}{r_0} + \frac{t_0^2}{2r_0^2}}\left(\frac{r_0 - \Delta t}{r_0}\right)^2\cdot\theta. \quad \text{(Eq 9)}$$

If the variation of wall thickness in the outer convex portion is neglected, namely $r \approx r_0$, Eq 9 can be simplified as

$$\Delta\theta = \frac{D}{E}\frac{1}{1 - 2\frac{t_0}{d_0} + 2\left(\frac{t_0}{d_0}\right)^2}\theta \quad \text{(Eq 10)}$$

From Eq 9 and 10, it is shown that if the tangential tensile force is considered while the movement of the NL is neglected, the springback angle $\Delta\theta$ increases linearly with the increase of the linear hardening coefficient D and the bending angle θ, and decreases with the increase of the elastic modulus E. Moreover, it is related to the wall thickness/diameter ratio t_0/d_0 of tube (Ref 20). The bending radius/diameter ratio R/d_0 is an important parameter that characterizes the severity of deformation. Because its effect is not considered in Eq 10, the calculated value of $\Delta\theta$ is far smaller than the experimental result. However, for a given tube, Eq 10 could predict the variation of $\Delta\theta$ with the wall thickness/diameter ratio. For 1Cr18Ni9Ti tube, 5A03 tube and T2 tube, substituting their parameters of materials properties and geometry into Eq 10, respectively, we can obtain the variation of springback angles $\Delta\theta$ with t_0/d_0. The corresponding curves are shown in Fig. 5. As presented in Fig. 5, the thinner the tube's wall, the smaller the springback angle is. When t_0/d_0 is relatively small (≤ 0.35), $\Delta\theta$ grows linearly with the accretion of t_0/d_0. When t_0/d_0 is >0.35, the growing gratitude of $\Delta\theta$ with t_0/d_0 gradually decreases. Particularly, when the wall thickness of tube increases to such an amount close to solid round bar ($t_0/d_0 \to 0.5$), the influence of the variation of t_0/d_0 on $\Delta\theta$ tends to stability.

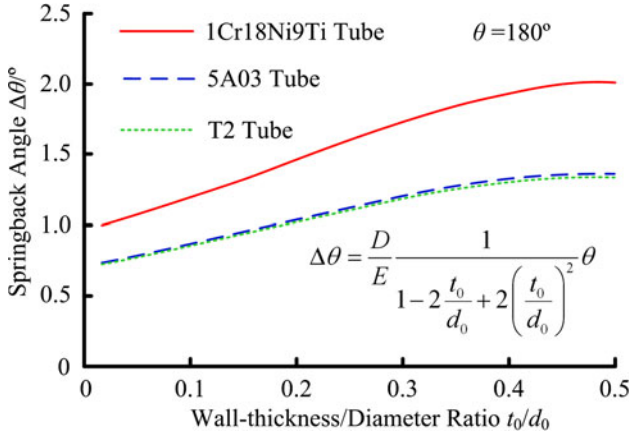

Fig. 5 The dependency of the springback angle on the wall thickness/diameter ratio for tubes with three materials

4.1.2 The Consideration of the Movement of the NL. Compared with pure bending, under the additional tensile force F, rotary draw bending increases the tangential tensile stress in the outer convex portion of tube and makes the whole tube add the component of tangential tension. When the tension is balanced with the tangential compression in the inner concave portion of tube, the NL will move toward the bending center. When the offset of the NL to the central layer is expressed by $\xi = r\sin\alpha$. As shown in Fig. 4, the tangential stress can be given as

$$\sigma_\theta = \sigma_y\left(1-\frac{D}{E}\right)+\sigma_F\frac{D}{E}+D\frac{r\sin\varphi + r\sin\alpha}{R-r\sin\alpha}. \quad \text{(Eq 11)}$$

With the movement of the NL, the arm of force in any point with the radius r can be expressed by $r\sin\varphi + r\sin\alpha$, and then the applied bending moment is

$$\begin{aligned} M &= \int_0^{2\pi}\sigma_\theta(r\sin\varphi + r\sin\alpha)r_m t\,d\varphi \\ &= \int_0^{2\pi}\left[\sigma_y\left(1-\frac{D}{E}\right)+\sigma_F\frac{D}{E}+D\frac{r\sin\varphi+r\sin\alpha}{R-r\sin\alpha}\right] \\ &\quad\times(r\sin\varphi + r\sin\alpha)r_m t\,d\varphi \\ &= r_m t r\left\{\left[\sigma_y\left(1-\frac{D}{E}\right)+\sigma_F\frac{D}{E}\right](2\pi\sin\alpha)+D\frac{\pi+2\pi\sin^2\alpha}{R/r-\sin\alpha}\right\}. \end{aligned} \quad \text{(Eq 12)}$$

Substituting Eq 7 and 12 into 6, we can obtain

$$\Delta\theta = \frac{D}{E}\frac{2\left(\sigma_y\frac{E-D}{DE}+\sigma_F\frac{1}{E}\right)(R/r-\sin\alpha)\sin\alpha+2\sin^2\alpha+1}{1-2\frac{t_0}{d_0}+2\left(\frac{t_0}{d_0}\right)^2}\times\left(1-\frac{\Delta t}{r_0}\right)^2\theta. \quad \text{(Eq 13)}$$

When the additional tensile force and the movement of the NL are considered, the springback angle $\Delta\theta$ is positively correlated with the material parameters including σ_y, D, and σ_F caused by the additional tensile force F and negatively with the elastic modulus E; it is positively correlated with the deformation parameters including θ, R/d_0 and t_0/d_0. In addition, $\Delta\theta$ decreases with wall thinning and increases with the accretion of the movement (indirectly denoted by the displacement angle α) of the NL toward the bending center. In fact, the latter two parameters are indirectly dependent on material properties and deformation conditions (Ref 21). If there is not significant ovalization on cross section of tube, the variation of wall thickness in the outer convex portion can be neglected, namely $r \approx r_0$, and then Eq 13 can be simplified as

$$\Delta\theta = \frac{D}{E}\frac{2\left(\sigma_y\frac{E-D}{DE}+\sigma_F\frac{1}{E}\right)\left(2\frac{R}{d_0}-\sin\alpha\right)\sin\alpha+2\sin^2\alpha+1}{1-2\frac{t_0}{d_0}+2\left(\frac{t_0}{d_0}\right)^2}\theta \quad \text{(Eq 14)}$$

According to Eq 14, because the value of $\sigma_y\frac{E-D}{DE}+\sigma_F\frac{1}{E}$ is <1, the springback angle $\Delta\theta$ will increase with the increase of the displacement angle α corresponding to the NL as material and other deformation conditions are given.

4.2 The Springback When $\varepsilon_F = \varepsilon_y$

When the tensile strain ε_F caused only by the tensile force F is equal to the strain ε_y corresponding to the original yield point, namely $\varepsilon_F = \varepsilon_y$, the compression deformation in the section below the central layer decreases due to the additional tensile force, and the movement of the NL toward the bending center increases to such an amount that could not be neglected. When $\sigma_F = \sigma_y$, the tangential stress will vary following A'_1A_1 lines shown in Fig. 3. And according to Eq 13, we can be obtain

$$\Delta\theta = \frac{2\frac{\sigma_y}{E}(R/r-\sin\alpha)\sin\alpha+\frac{D}{E}(2\sin^2\alpha+1)}{1-2\frac{t_0}{d_0}+2\left(\frac{t_0}{d_0}\right)^2}\left(1-\frac{\Delta t}{r_0}\right)^2\theta. \quad \text{(Eq 15)}$$

When other deformation conditions keep constant, the springback angle $\Delta\theta$ will decrease with the accretion of the wall thinning amount Δt in the outer convex portion of tube. If it is approximately valid that $r = r_0$, Eq 15 can be further simplified as

$$\Delta\theta = \frac{2\frac{\sigma_y}{E}\left(2\frac{R}{d_0}-\sin\alpha\right)\sin\alpha+\frac{D}{E}(2\sin^2\alpha+1)}{1-2\frac{t_0}{d_0}+2\left(\frac{t_0}{d_0}\right)^2}\theta. \quad \text{(Eq 16)}$$

When the movement of the NL is neglected, namely $\alpha = 0$, Eq 16 have an identical structure with Eq 10. Figure 6 describes the dependences of the springback angles $\Delta\theta$ calculated with numerical method on the displacement angle α of the NL, which involve the tubes with three different materials on the same deformation conditions. From it, the springback angle $\Delta\theta$ is positively correlated with the displacement angle α. When $\alpha \le 60°$, the variation $\Delta\theta$ with α is approximately linear; when $\alpha > 60°$, the variation gradient decreases gradually; when α is close to 90°, $\Delta\theta$ does not vary with the accretion of α. In fact, for the hardening material, when $\varepsilon_F = \varepsilon_y$, it is impossible that the NL moves to the inner concave surface of tube where $\alpha = 90°$, and thus it is no practical sense to calculate the value of $\Delta\theta$ as $\alpha = 90°$. Also, according to Fig. 6, when other conditions keep changeless, $\Delta\theta$ increases with the accretion of R/d_0, and the greater the movement (α) of the NL, the more significant the growing tendency of $\Delta\theta$ with R/d_0 is.

In addition, from Fig. 6, it is found that the influence of R/d_0 on $\Delta\theta$ depends on material properties, and in the three tubes, the

variation of $\Delta\theta$ with R/d_0 for 5A03 tube is the largest, while that for T2 tube is the smallest. This is because σ_y/E and R/d_0 in $4\frac{\sigma_y}{E}\frac{R}{d_0}\sin\alpha$ of Eq 16 interact with each other and when the value of R/d_0 is same, the greater the value of σ_y/E is, the greater the springback angle $\Delta\theta$ is. The values of σ_y/E for 5A03, 1Cr18Ni9Ti, and T2 are 1.035×10^{-3}, 1.095×10^{-3}, and 0.636×10^{-3}, respectively. Therefore, the sensitivity of $\Delta\theta$ to R/d_0 is the strongest for 5A03 while that is the weakest for T2.

Based on the experimental results of the springback angle, the movement of the NL can be reversely calculated following Eq 14 and 16. However, the calculation process is too complex to present in the article.

4.3 The Springback when $\varepsilon_F > \varepsilon_y$

When the strain ε_F continues to increase and its absolute value is equal to the amount of elastic component of tangential compress deformation in the inner concave portion of tube, the distribution of stress in the transverse section of tube in Fig. 3 will be turned into A'_2A_2 lines. In the inner concave surface of tube, the tangential tensile deformation caused by the additional tensile force F could balance the tangential compress deformation caused by the bending moment, and the NL may move to the inner concave surface of tube. And at the moment, the tangential strain of the longitudinal fiber on the inner concave surface can be expressed as

$$\varepsilon_\theta = \varepsilon_F + \frac{r\sin\varphi}{\rho} = \varepsilon_F + \frac{r\sin\varphi}{R_i} = 0 \qquad \text{(Eq 17)}$$

where R_i is the curvature radius of the inner concave surface of tube.

According to Eq 17, the tangential deformation (nominal strain) caused by tensile force F on the inner concave surface could be obtained as

$$\varepsilon_F = -\frac{r\sin\varphi}{\rho} = -\frac{r\sin\left(\frac{3}{2}\pi\right)}{R_i} = \frac{r}{R_i}. \qquad \text{(Eq 18)}$$

In fact, all longitudinal fibers of tube are subjected to such the tangential tensile deformation. Besides the inner concave surface, the whole tube endures the tangential tensile deformation, and under the combined bending moment and additional tensile force, the tangential strain in any a point with the radius r can be expressed by

$$\varepsilon_\theta = \frac{r}{R_i}(1+\sin\varphi). \qquad \text{(Eq 19)}$$

The corresponding tangential stress can be represented as

$$\sigma_\theta = \sigma_y + D\varepsilon_\theta = \sigma_y + D\frac{r}{R_i}(1+\sin\varphi). \qquad \text{(Eq 20)}$$

The applied bending moment is

$$M = \int_0^{2\pi} \sigma_\theta r_m t\,d\varphi(r + r\sin\varphi) = r_m t r\pi\left(2\sigma_y + 3D\frac{r}{R_i}\right). \qquad \text{(Eq 21)}$$

Substituting Eq 21 and 7 into 6, we can get the springback angle as follows:

$$\Delta\theta = \frac{2\frac{\sigma_y}{E}\left(2\frac{R}{d_0}-1\right) + 3\frac{D}{E}\left(1-\frac{\Delta t}{r_0}\right)}{1-2\frac{t_0}{d_0}+2\left(\frac{t_0}{d_0}\right)^2}\left(1-\frac{\Delta t}{r_0}\right)\theta. \qquad \text{(Eq 22)}$$

As mentioned above, the springback angle $\Delta\theta$ decreases with the accretion of the wall thinning amount Δt in the outer convex portion of tube. If the variation of wall thickness is neglected, namely $r = r_0$, Eq 22 can be simplified as

$$\Delta\theta = \frac{2\frac{\sigma_y}{E}\left(\frac{2R}{d_0}-1\right) + 3\frac{D}{E}}{1-2\frac{t_0}{d_0}+2\left(\frac{t_0}{d_0}\right)^2}\theta \qquad \text{(Eq 23)}$$

Equation 23 shows that when the NL moves to the inner concave surface due to the additional tensile force, the springback angle $\Delta\theta$ has the approximately linear relationship with the parameters of material properties. Specifically, it is positively correlated with the original yield stress σ_y and the plastic coefficient D, and negatively correlated with the elastic modulus E. In addition, $\Delta\theta$ increases linearly with the accretion of the bending angle θ and the bending radius/diameter ratio R/d_0, and similar to the calculated results by Eq 10, it has a growing tendency with the accretion of t_0/d_0. To validate the calculations, some calculated results are compared with the corresponding experimental data and simulation results as shown in Fig. 7.

If it is a consideration that the NL moves to the inner concave surface, comparison between the variation tendencies

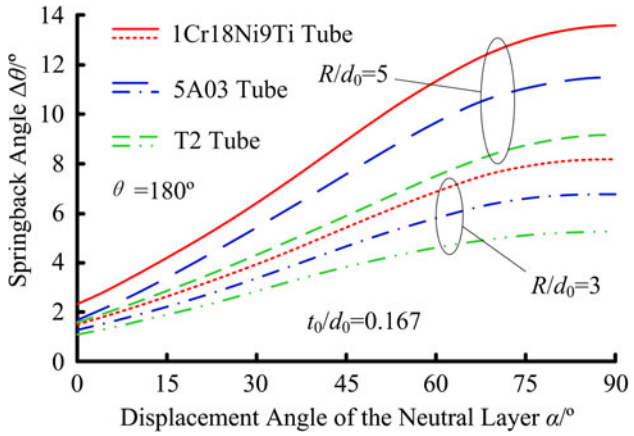

Fig. 6 The variation of the springback angle with the accreting of the movement of the NL

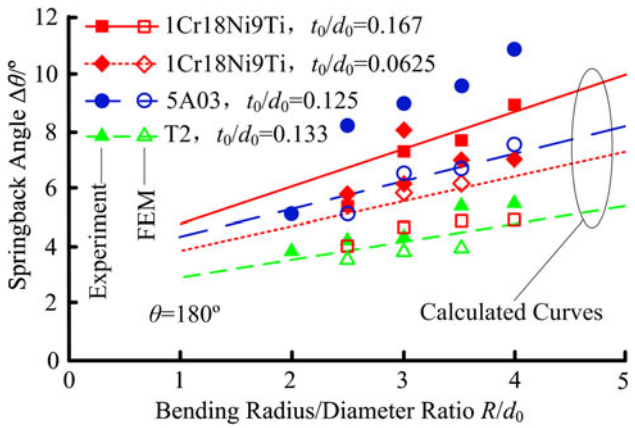

Fig. 7 The variation of the springback angle with the bending radius/diameter ratio

of the calculated values and the experimental data of $\Delta\theta$ shows very good agreement. Particularly, for 1Cr18Ni9Ti tube and T2 tube, the calculated results agree well with the experimental data. However, when the wall thickness/diameter ratio is small ($t_0/d_0 = 0.0625$), for 1Cr18Ni9Ti tube, the experimental data of $\Delta\theta$ that vary irregularly are significantly greater than the calculated value. For T2 tube, the calculated values of $\Delta\theta$ are located between the experimental data and the FEM results. For 5A03 tube, the calculated values of $\Delta\theta$ are close to the FEM results, and far lower than experimental data. This would be a major issue in our successive research.

5. Conclusions

(1) When the tangential tensile strain $\varepsilon_F < \varepsilon_y$, with the movement of the NL neglected, the calculated value of the springback angle is very small compared with the experimental data. The calculated curves show that the springback angle increases with larger wall thickness/diameter ratio of tube. However, when the ratio increases to the amount related to the solid round bar, the influence of increasing wall thickness on the springback angle becomes very weak. If the movement of the NL is considered, besides the above-stated factors, the springback angle increases with the accretion of the original yield stress, the tangential stress caused by the additional tensile force and the bending radius/diameter ratio. Moreover, the greater the movement of the NL, the greater will be the springback angle. The springback angle decreases with the accretion of the wall thinning amount.

(2) When the tangential tensile strain $\varepsilon_F = \varepsilon_y$, with the movement of the NL increasing, the springback angle increases remarkably. However, as the NL moves to the inner concave surface, the variation gradient gradually decreases. Especially, when the movement of the NL is relatively large, the springback angle will significantly increase with larger bending radius/diameter ratio, and the increase depends on material properties, namely the greater the ratio of the original yield stress to the elastic modulus, the greater will be the growing amount with the accretion of the bending radius/diameter ratio.

(3) When the additional tensile force increases to such an amount that $\varepsilon_F > \varepsilon_y$ and the tangential tensile strain is numerically equal to the elastic compressive strain caused by pure bending moment on the inner concave surface, the two strains will counteract each other and the whole tube will endure the tangential tensile deformation except at the inner concave surface and the NL will move to the surface. The springback angle $\Delta\theta$ is positively proportional to the original yield stress and the plastic coefficient, and inversely proportional to the elastic modulus. In addition, $\Delta\theta$ increases linearly with the accretion of the bending angle and the bending radius/diameter ratio. Also it increases with the accretion of the wall thickness/diameter ratio, and its growing tendency becomes significant with the increase of the bending radius/diameter ratio.

Since the influence of the additional tensile force is considered, the mechanical model between pure bending and draw-bending should obey the work principle of modern NC tube bender. Therefore, the analysis methods presented in the article could provide reference for predicting and compensating springback in NC tube bending.

Acknowledgments

This research is based upon work supported by Capital Aerospace Machinery Company and Beijing Satellite Manufacturing Factory. The authors wish to gratefully acknowledge these supports.

References

1. S. Kyriakides, E. Corona, and J.E. Miller, Effect of Yield Surface Evolution on Bending Induced Cross Sectional Deformation of Thin-Walled Sections, *Int. J. Plast*, 2004, **20**, p 607–618
2. E. Corona and S.E. Vaze, Buckling of Elastic-Plastic Square Tubes Under Bending, *Int. J. Mech. Sci.*, 1996, **38**, p 735–755
3. Z. Jin, S. Luo, and X. Daniel, KBS-Aided Design of Tube Bending Processes, *Eng. Appl. Artif. Intel.*, 2001, **14**, p 599–606
4. N.C. Tang, Plastic-Deformation Analysis in Tube Bending, *Int. J. Press. Vessel Pip.*, 2000, **77**, p 751–759
5. K. Trana, Finite Element Simulation of the Tube Hydroforming Process—Bending Performing and Hydroforming, *J. Mater. Process. Technol.*, 2002, **127**, p 401–408
6. Y.C. Liu and M.L. Day, Bending Collapse of Thin-Walled Circular Tubes and Computational Application, *Thin Walled Struct.*, 2008, **46**, p 442–450
7. H.A. AI-Qureshi, Elastic-Plastic Analysis of Tube Banding, *Int. J. Mach. Tools Manuf*, 1999, **39**, p 87–104
8. H.A. AIQureshi and A. Russo, Spring-back and Residual Stresses in Bending of Thin-Walled Aluminum Tubes, *Mater. Des.*, 2002, **23**, p 217–222
9. R.M. Cleveland and A.K. Ghosh, Inelastic Effects on Springback in Metals, *Int. J. Plast*, 2002, **18**, p 769–785
10. L. Luo and A.K. Ghosh, Elastic and Inelastic Recovery After Plastic Deformation of DQSK Steel Sheet, *J. Eng. Mater. Technol.*, 2003, **125**, p 238–246
11. A. Megharbel, G.A. Nasser, and A. Domiaty, Bending of Tube and Section Made of Strain-Hardening Materials, *J. Mater. Process. Technol.*, 2008, **203**, p 372–380
12. M. Murata, T. Kuboki, and K. Takahashi, Effect of Hardening Exponent on Tube Bending, *J. Mater. Process. Technol.*, 2008, **201**, p 189–192
13. D.X. E and Y.F. Liu, Springback and Time-Dependent Springback of 1Cr18Ni9Ti Stainless Steel Tubes Under Bending, *Mater. Des.*, 2010, **31**, p 1256–1261
14. D.X. E, R.X. Ning, and C.T. Tang, The Experimental and Spring Back Analysis of Rotary Draw Tube Bending, *Beijing. Inst. Technol.*, 2006, **26**, p 410–412, 432 (in Chinese)
15. D.X. E, M. Takaji, and Z.G. Li, Stress Analysis of Rectangular Cup Drawing, *J. Mater. Process. Technol.*, 2008, **205**, p 469–476
16. D.X. E, H. He, X. Liu, and R.X. Ning, Experimental Study and Finite Element Analysis of Spring-back Deformation in Tube Bending, *Int. J. Miner. Metall. Mater.*, 2009, **2**, p 177–183
17. D.X. E, R.X. Ning, and Y.M. Li, Experimental Study on the Wall Thickness Thinning of the Curved Tube Affected by Material Property, *Mater. Sci. Technol.*, 2008, **2**, p 200–203 (in Chinese)
18. D.X. E and X.F. Wang, Plane Stress Analysis of Tube-Bending Flatting and Relative Bending Radius, *Plast. Eng.*, 2007, **14**, p 25–28 (in Chinese)
19. D.X. E, X.D. Guo, and R.X. Ning, Analysis on the Strain Neutral Layer Displacement in Tube-Bending Process, *Chin. J. Mech. Eng.*, 2009, **3**, p 207–310 (in Chinese)
20. D.X. E and M.F. Chen, Numerical Solution of Thin-Walled Tube Bending Springback With Exponential Hardening Law, *Steel. Res. Int.*, 2010, **81**, p 286–291
21. D.X. E, R.X. Ning, and T. Gu, Analysis on the Elastic-Plastic Deformation During Tube-Bending Process, *Acta Armamentarii*, 2009, **10**, p 17–20 (in Chinese)